

Accurate closed-form solution of the SIR epidemic model

Nathaniel S. Barlow¹ and Steven J. Weinstein^{1,2}

¹*School of Mathematical Sciences, Rochester Institute of Technology, Rochester, NY 14623, USA*

²*Department of Chemical Engineering, Rochester Institute of Technology, Rochester, NY 14623, USA*

(Dated: 22 December 2024)

An accurate closed-form solution is obtained to the SIR Epidemic Model through the use of Asymptotic Approximants (Barlow et. al, 2017, Q. JI Mech. Appl. Math, 70 (1), 21-48). The solution is created by analytically continuing the divergent power series solution such that it matches the long-time asymptotic behavior of the epidemic model. The utility of the analytical form is demonstrated through its application to the COVID-19 pandemic.

There are several problems of mathematical physics in which the only available analytic solution is a divergent and/or truncated series expansion. Over the past decade, a new approach has evolved to overcome the convergence barrier in series solutions. An asymptotic approximant is a closed-form analytic expression whose expansion in one region is exact up to a specified order and whose asymptotic equivalence in another region is enforced. The remarkable feature of asymptotic approximants is their ability to attain uniform accuracy not only at the two regions enforced, but also at all points in-between, as demonstrated thus far for problems in thermodynamics, astrophysics, and fluid dynamics¹⁻⁷. The current need to model and predict viral epidemics motivates us to extend the application of asymptotic approximants to the commonly used Susceptible-Infected-Recovered (SIR) model. This model is formulated as a system of nonlinear ordinary differential equations, and has no analytic solution. Interestingly, the SIR model shares the same asymptotic features as boundary layer flow over a moving flat plate, for which asymptotic approximants have already been applied⁴. The analytic nature of the asymptotic approximant derived in what follows is advantageous. Model parameters may be extracted for available COVID-19 data via a least squares (or equivalent) technique without the need for an embedded numerical scheme.

The SIR epidemic model considers the time-evolution of a susceptible population, $S(t)$, interacting with an infected population, $I(t)$, where t is time. This model is expressed as⁸

$$\frac{dS}{dt} = -rSI \quad (1a)$$

$$\frac{dI}{dt} = rSI - \alpha I \quad (1b)$$

with constraints

$$S = S_0, I = I_0 \text{ at } t = 0, \quad (1c)$$

where r , α , S_0 , I_0 are non-negative constant parameters⁸. Once (1) is solved, the recovered population is extracted as:

$$R(t) = \alpha \int_0^t I(\zeta) d\zeta. \quad (2)$$

Equation (1a) can be thought of as a standard collision model in a 2nd-order chemical reaction, where species S and I “collide” to deplete the population of S to create the species I . In this interpretation, r is a rate constant, which in practice may be reduced by population behavior such as “social distancing”. In the case where $\alpha=0$ in (1b), the system (1) indicates that $S + I = S_0 + I_0$ for all time. For $\alpha \neq 0$, then, (1b) indicates that the number of infected are reduced in time, and it is seen that the parameter α determines the rate of recovery of infected individuals. The omission of a negative $\alpha I(t)$ term in (1a) is an implicit model assumption that the recovered population is no longer susceptible to the disease.

We now manipulate the system (1) into an equivalent first-order equation to simplify the analysis that follows. Equations (1a) and (1b) are divided to obtain

$$\frac{dI}{dS} = \frac{\alpha}{rS} - 1. \quad (3)$$

Subsequent integration of (3) with respect to S and application of the constraints (1c) yields

$$I = \frac{\alpha}{r} \ln \left(\frac{S}{S_0} \right) - S + S_0 + I_0. \quad (4)$$

Equation (4) is substituted into equation (1a) to obtain

$$\frac{dS}{dt} = \beta S + rS^2 - \alpha S \ln S \quad (5a)$$

where

$$\beta = \alpha \ln S_0 - r(S_0 + I_0). \quad (5b)$$

From equation (1c), the constraint on S is:

$$S = S_0 \text{ at } t = 0. \quad (5c)$$

Equation (5) is equivalent to the system (1) to solve for S and, once solved, the solution for I may be obtained using (4), which may be integrated to find R from (2).

The series solution of (5) is given by

$$S = \sum_{n=0}^{\infty} a_n t^n, \quad a_0 = S_0 \quad (6a)$$

$$a_{n+1} = \frac{1}{n+1} \left[\beta a_n + \sum_{j=0}^n a_j (r a_{n-j} - \alpha b_{n-j}) \right], \quad (6b)$$

$$b_{n>0} = \frac{1}{n} \sum_{j=0}^{n-1} a_{j+1} \tilde{a}_{n-1-j}, \quad b_0 = \ln a_0, \quad (6c)$$

$$\tilde{a}_{n>0} = \frac{-1}{a_0} \sum_{j=1}^n a_j \tilde{a}_{n-j}, \quad \tilde{a}_0 = \frac{1}{a_0}. \quad (6d)$$

The result (6) is obtained by applying Cauchy's product rule⁹ to expand S^2 and $S \ln S$ in (5). The expansion of $\ln S$ is obtained by first applying Cauchy's product rule to the identity $SS^{-1} = 1$ and evaluating like-terms to obtain a recursive expression for the coefficients of the expansion of S^{-1} , given by (6d). The expansion of S^{-1} is subsequently integrated term-by-term to obtain the expansion of $\ln S$, whose coefficients are given by (6c). Although the series solution given by (6) is an analytic solution to (5), it is only valid within its radius of convergence and is incapable of capturing the long-time behavior of S . This motivates the construction of an approximant to analytically continue the series beyond this convergence barrier.

The long-time asymptotic behavior of the system (5) is required to develop our asymptotic approximant, and so we proceed as follows. It has been proven in prior literature¹⁰ that S approaches a limiting value, S_∞ , as $t \rightarrow \infty$, and this corresponds to $I \rightarrow 0$ according to (5). The value of S_∞ satisfies equation (4) with $I = 0$ as¹⁰

$$\frac{\alpha}{r} \ln \left(\frac{S_\infty}{S_0} \right) - S_\infty + S_0 + I_0 = 0. \quad (7)$$

We expand S as $t \rightarrow \infty$ as follows:

$$S \sim S_\infty + S_1(t) \text{ where } S_1 \rightarrow 0 \text{ as } t \rightarrow \infty. \quad (8)$$

Equation (8) is substituted into (5) and terms of $O(S_1^2)$ are neglected to achieve the following linearized equation

$$\frac{dS_1}{dt} = \kappa S_1 \quad (9a)$$

where

$$\kappa = rS_\infty - \alpha. \quad (9b)$$

In writing exponent (9b), the definition of β in (5b) has been used. Additionally, to obtain (9), equation (7) has been used which eliminates all $O(1)$ terms in the linearized system. The solution to (9) is

$$S_1 = \varepsilon e^{\kappa t}, \quad (10)$$

where ε is an unknown constant that can only be determined via connection with short-time behavior. Consistent with the assumptions made, we find $\kappa < 0$ such

that $S_1 \rightarrow 0$ as $t \rightarrow \infty$. Thus the long-time asymptotic behavior of S is given by

$$S \sim S_\infty + \varepsilon e^{\kappa t}, \quad t \rightarrow \infty. \quad (11)$$

Higher order corrections to the expansion (11) may be obtained by the method of dominant balance¹¹ as a series of more rapidly damped exponentials of the form $e^{n\kappa t}$ where $n > 1$. This long-time asymptotic behavior of successive exponentials mimics that of the Sakiadis boundary layer problem describing flow along a moving plate in a stationary fluid⁴. It is natural then, to apply the Sakiadis approximant⁴ to capture this asymptotic behavior while retaining the $t = 0$ behavior given by (6a). The Sakiadis approximant imposes the exponential form of the long-time asymptotic behavior (11) for all time; the coefficients of the exponentials are determined by matching their short-time expansion to the known power series developed about $t = 0$ in the form of (6a). However, here we find that a reciprocal form that achieves the same $t \rightarrow \infty$ behavior (11) (through its binomial expansion) converges faster than the original Sakiadis approximant.

The assumed SIR approximant is given by

$$S_{A,N} = \frac{S_\infty}{1 + \sum_{n=1}^N A_n e^{n\kappa t}} \quad (12a)$$

where the A_n 's are obtained by taking the reciprocal of both sides of (12a), expanding each side about $t = 0$, and equating like-terms. The coefficients of the subsequent reciprocal expansion of the left-hand side (that of S^{-1}) are given by (6d). After equating like-terms of this expansion with that of the reciprocal of the right-hand side of (12a), one arrives at the following linear system of equations to solve for the A_n values as

$$\begin{bmatrix} 1^0 & 2^0 & 3^0 & \dots & N^0 \\ 1^1 & 2^1 & 3^1 & \dots & N^1 \\ 1^2 & 2^2 & 3^2 & \dots & N^2 \\ \vdots & \vdots & \vdots & \vdots & \vdots \\ 1^{N-1} & 2^{N-1} & 3^{N-1} & \dots & N^{N-1} \end{bmatrix} \begin{bmatrix} A_1 \\ A_2 \\ A_3 \\ \vdots \\ A_N \end{bmatrix} = \vec{f}, \quad (12b)$$

$$\vec{f} = S_\infty \begin{bmatrix} 0! \tilde{a}_0 + 2\kappa/S_\infty \\ 1! (-1/\kappa) \tilde{a}_1 \\ 2! (-1/\kappa)^2 \tilde{a}_2 \\ \vdots \\ (N-1)! (-1/\kappa)^{N-1} \tilde{a}_{N-1} \end{bmatrix}, \quad (12c)$$

where (12b) is a Vandermonde matrix whose inversion is explicitly known¹³. The SIR approximant (12) is thus a closed-form expression that, by construction, matches the correct $t \rightarrow \infty$ behavior given by (11) and whose expansion about $t = 0$ is exact to N^{th} -order.

Figure 1a provides a typical comparison of the N -term series solution (6) denoted by $S_{S,N}$ (and dashed lines), the N -term approximant (12) denoted by $S_{A,N}$ (solid

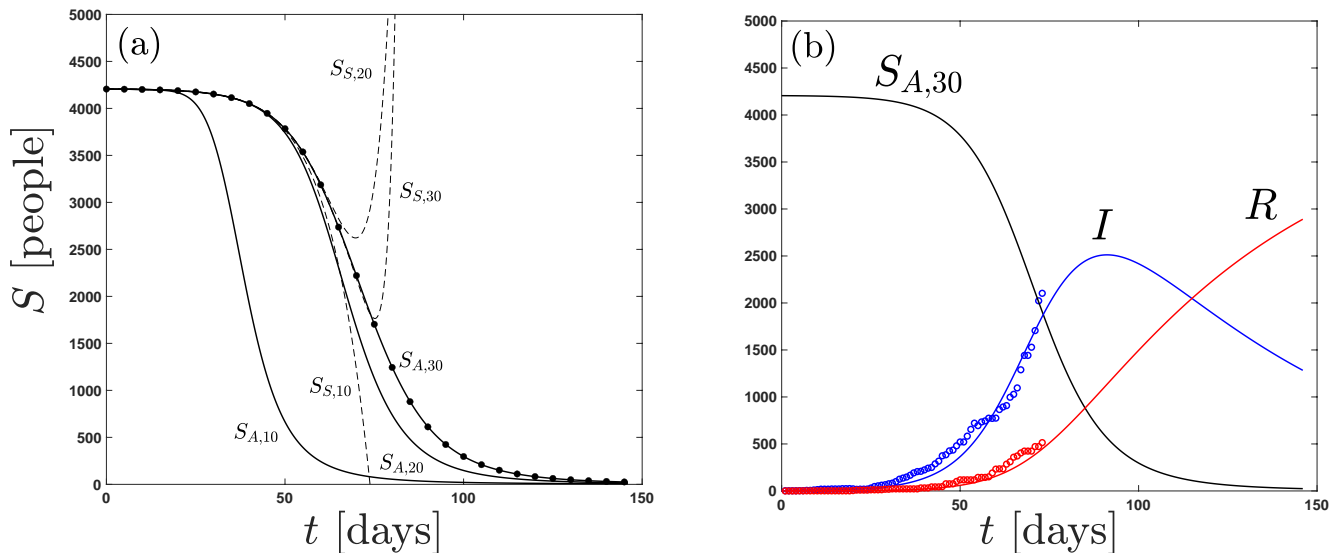


FIG. 1. Analytical and numerical solutions to the SIR model (5), showing the susceptible population S versus time. (a) As the number of terms N is increased, the series solution, denoted $S_{S,N}$ (given by (6a)), diverges and the approximant, denoted $S_{A,N}$ (given by (12)), converges to the exact (numerical) solution (\bullet 's). (b) The converged approximant for S is used to obtain R and I (from equations (2) and (4), respectively), and is compared with data¹² (\circ 's) from the Italy COVID-19 outbreak where $t = 0$ is January 22, 2020. The model parameters values $\alpha=0.0164$ and $r=2.9236 \times 10^{-5}$ were obtained via a least-squares fit between the approximant and the outbreak data, using initial conditions $I_0 = 2$ (from the first point in the data set¹²) and $S_0 = 4206$.

lines), and the numerical solution (indicated by symbols). Note that the series solution has a finite radius of convergence as evidenced by the poor agreement and divergence from the numerical solution at larger times, even as additional terms are included. By contrast, the approximant converges as additional terms are included. For $N = 30$, the approximate is visibly indistinguishable from the numerical solution (obtained by forward differencing) with a maximum relative error on the order of the numerical time-step (here 10^{-2}) over the time range indicated. Increasing the number of terms beyond $N = 30$ does improve accuracy up to a point, but also increases the likelihood of deficient approximants for which the denominator can be zero for certain time values and specific values of N . In general, the lowest number of terms that yields the desired accuracy is chosen to avoid this behavior. The convergence of the approximant with increasing N is a necessary condition for valid approximant. For the problems of mathematical physics to which we have applied asymptotic approximants¹⁻⁷, we have observed that convergence of approximants implies excellent agreement with numerical results. There is as of yet no proof developed that guarantees this result, but this interesting behavior has thus been a property of all approximants developed thus far.

Figure 1b provides an application of the 30-term approximant ($S_{A,30}$) to COVID-19 data for Italy¹², indicated by plot symbols. The data¹² is reported in terms of confirmed cases and recovered individuals per day; the infected population, I , is taken as difference between these

two quantities. A least squares fit of the approximant to I is used to extract parameters α and r based on data from the initial stages of the COVID-19 epidemic in Italy. To do so, (4) is used to relate I analytically to the solution for S (here, the approximant $S_{A,30}$); note that S_∞ , used in the approximant, is affected by these parameters explicitly according to (7). The value of S_0 is not provided in the data set¹², and a least-squares algorithm is ineffective at determining an optimal value. Here, we choose the value of S_0 to be twice that of the maximum value of I from the data, as it captures a typical curve shape for S seen in applications of the SIR model¹⁰. In regards to the sensitivity of fitting parameters to the choice for S_0 , a 100% difference in S_0 leads to roughly a 50% difference in r and a 6% difference in α . The fit is made especially simple owing to the analytical form of the approximant that obviates the need to imbed the numerical solution in such an algorithm. The plot of the population of recovered individuals, R versus t , is extracted from the solution for I by direct integration in accordance with (2). Note that the predicted curve for R , obtained solely by fitting data for I , is in good agreement with COVID data for the recovered population, and serves as a check on the consistency of the data and algorithm here.

The plot in figure 1b indicates how the initial stages of the disease progression may be used to predict the peak in the number of infected and recovered individuals. At the time of this analysis being performed, the duration of the epidemic has not been long enough to examine whether the model is predictive of this feature.

Nevertheless, whether the SIR model is predictive for the epidemic is an assessment of the model itself, and not the efficacy of the closed-form approximant developed here. Future work may focus on whether asymptotic approximants may be used to develop closed-form solutions for more sophisticated epidemic models. The SIR approximant demonstrates the potential of this approach to such problems and warrants further study.

¹N. S. Barlow, A. J. Schultz, S. J. Weinstein, and D. A. Kofke, *J. Chem. Phys.* **137**, 204102 (2012).

²N. S. Barlow, A. J. Schultz, S. J. Weinstein, and D. A. Kofke, *AIChE J.* **60**, 3336 (2014).

³N. S. Barlow, A. J. Schultz, S. J. Weinstein, and D. A. Kofke, *J. Chem. Phys.* **143**, 071103:1 (2015).

⁴N. S. Barlow, C. R. Stanton, N. Hill, S. J. Weinstein, and A. G. Cio, *Q. J. Mech. Appl. Math.* **70**, 21 (2017).

⁵N. S. Barlow, S. J. Weinstein, and J. A. Faber, *Class. Quant. Grav.* **34**, 1 (2017).

⁶R. J. Beachley, M. Mistysyn, J. A. Faber, S. J. Weinstein, and N. S. Barlow, *Class. Quant. Grav.* **35**, 1 (2018).

⁷E. R. Belden, Z. A. Dickman, S. J. Weinstein, A. D. Archibee, E. Burroughs, and N. S. Barlow, *Q. J. Mech. Appl. Math.* **73**, 36 (2020).

⁸W. O. Kermack and A. G. McKendrick, *Proc. Roy. Soc. London A* **115**, 700 (1927).

⁹R. V. Churchill, *Complex Variables* (McGraw-Hill, 1948).

¹⁰H. W. Hethcote, *SIAM Rev.* **42**, 599 (2000).

¹¹C. M. Bender and S. A. Orszag, *Advanced Mathematical Methods for Scientists and Engineers I: Asymptotic Methods and Perturbation Theory* (McGraw-Hill, 1978).

¹²John Hopkins University CSSE, "Novel coronavirus (covid-19) cases," <https://github.com/CSSEGISandData/COVID-19>.

¹³L. R. Turner, "Inverse of the Vandermonde matrix with applications," Technical Note D-3547 (NASA, 1966).